



# Surface Engineering Design of Alumina-Matrix Composites

# 9

Yongsheng Zhang, Hengzhong Fan, Litian Hu, Yuan Fang, and  
Junjie Song

## Contents

9.1 Introduction .....	242
9.2 Laser Surface Texturing and Tribological Properties of Ceramic Composites .....	244
9.3 Surface Lubricating Design, Fabrication, and Tribological Properties in a Water Environment of Al <sub>2</sub> O <sub>3</sub> /Ni-Laminated Composites .....	248
9.4 Surface Lubricating Design, Fabrication, and Tribological Properties Under a Wide-Range Temperature of Al <sub>2</sub> O <sub>3</sub> /Mo-Laminated Composites .....	252
References .....	258

## Abstract

The three-dimensional lubricating layer on a ceramic surface realizes the integration of the structure and lubricating function in ceramic materials, which can achieve outstanding lubricating properties and maintain the excellent mechanical properties of ceramics, solving the special lubrication and wear failure in mechanical systems under extreme conditions (e.g., corrosive environment and wide-temperature range condition). In this chapter, two kinds of surface-lubricating structural-laminated ceramics with high reliability were designed and prepared based on experiment research and theoretical simulation. These ceramics can achieve stable and effective lubrication in a water environment and wide-temperature range condition. These materials are Al<sub>2</sub>O<sub>3</sub>/Ni- and

Y. Zhang (✉) · L. Hu · Y. Fang

State Key Laboratory of Solid Lubrication, Lanzhou Institute of Chemical Physics, Chinese Academy of Sciences, Lanzhou, China

H. Fan · J. Song

State Key Laboratory of Solid Lubrication, Lanzhou Institute of Chemical Physics, Chinese Academy of Sciences, Lanzhou, China

University of Chinese Academy of Sciences, Beijing, China

© Springer-Verlag GmbH Germany, part of Springer Nature 2022

P. L. Menezes et al. (eds.), *Self-Lubricating Composites*,

[https://doi.org/10.1007/978-3-662-64243-6\\_9](https://doi.org/10.1007/978-3-662-64243-6_9)

241

$\text{Al}_2\text{O}_3/\text{Mo}$ -laminated composites suitable for use in a water environment and in wide-temperature range conditions, respectively. The relation between the surface microstructure of the prepared materials and their properties (mechanical and tribological) was investigated. Results indicated that the integration of the structure and lubricating function of the ceramic composites is realized through the bionic, surface microstructure, and three-dimensional self-lubricating design of the materials, further improving their lubricating and practical properties. Factors that can influence the tribological behavior and wear failure of the above materials were proposed through the systematic study of the tribological behavior under different environments and test conditions, as well as the relation among the structure, composition, and properties of these two kinds of materials. In addition, theoretical models of the relation between the structural parameters and performance of the materials were built. These methods provided theories and technologies for the preparation and application of high performance lubricating materials that can be used in corrosive and wide-temperature range environments.

---

## 9.1 Introduction

Lubrication in extreme environment is a key factor that affects the security, high efficiency, and stable operation of a mechanical system. This factor also restricts the development of high-end equipment. During the past decades, various self-lubricating materials have been developed for different machineries. These developments were geared toward improving the properties of materials, allowing them to surmount severe challenges under extreme conditions. The lubricating materials for different fields must be capable of working in corrosive environments or other extreme conditions (e.g., wide-temperature range condition requires continuous and complex multienvironment lubrications) for a long time. In the current science and technology development context, high-performance ceramic lubricating materials are the most promising candidates for the harsh environment application of wear-resistant components because of their excellent mechanical properties, such as high strength, resistance to corrosion, and oxidation stability under extreme conditions, and insensitivity to defects. Moreover, ceramic lubricating composites are the only material that can work above 1000 °C and in complex harsh environments [1–6]. Nevertheless, the high friction coefficient of this kind of material under dry sliding, boundary lubrication conditions, and brittleness of the ceramic matrix itself limit their practical application in tribological and high-end equipment areas. Therefore, the design and fabrication of high-performance lubricating materials must be geared toward improving both the mechanical and lubricating properties. This can also solve the limited application of ceramic lubricating materials.

Laminating composites is one of the new strategies. The method integrates strong or weak interfaces with ceramics inspired by bionic multilayer structures, such as shells, lignum, and teeth. It has attracted significant research attention because of the excellent mechanical properties of structured ceramics. These materials possess

noncatastrophic fracture behavior and damage tolerance that exhibit much higher fracture toughness and work of fracture than monolithic ceramics [7–9]. The pioneering work of Clegg et al. successfully fabricated SiC/graphite-laminated composites using SiC as the strong layers and graphite as the weak interface. These materials exhibited great mechanical properties with a fracture toughness and work of fracture of  $15 \text{ MPa} \cdot \text{m}^{1/2}$  and  $4625 \text{ J} \cdot \text{m}^{-2}$ , respectively. Moreover, the laminated composites also showed excellent lubricating property and wear resistance because of their special weak interfacial graphite layer [10]. According to previous studies,  $\text{Al}_2\text{O}_3/\text{Ni}$  and  $\text{Al}_2\text{O}_3/\text{Mo}$  are typical laminated composites.  $\text{Al}_2\text{O}_3/\text{Ni}$  and  $\text{Al}_2\text{O}_3/\text{Mo}$  are promising candidates in corrosive environment and high temperature condition applications, respectively. The two typical laminated composites exhibit excellent mechanical properties that can achieve security, high efficiency, and stable operation for mechanical systems as structural materials [11, 12]. Nevertheless, the friction coefficient and wear rate of  $\text{Al}_2\text{O}_3/\text{Ni}$ -laminated composites are high and unstable under boundary lubricating conditions. The room and medium-temperature friction coefficients of  $\text{Al}_2\text{O}_3/\text{Mo}$ -laminated composites are high under dry sliding conditions. Thus, these factors limit the application of these two laminated composites in lubricating areas.

Laser surface texturing (LST), which forms regular micro-patterns on the sliding surface, is generally recognized as an effective means to improve the tribological property of moving part surfaces. Previous studies showed that the introduction of specific texturing on sliding surfaces can effectively alleviate the friction and wear of materials, increase the lifetime of the sliding contacts by trapping wear debris, or promote the retention of a lubricant film between mating surfaces [13–18]. This method combined with laser surface texture and solid lubricant films can significantly improve the tribological performance of materials. The mechanism of such composition-lubrication structure involves the use of textured microdimples on the material surface to store lubricants. Lubricants are squeezed on the friction surface to form a lubricating film during friction. This method improves the contact states between the friction pair. This process leads to reduced frictional wear and increased service life of materials. The method of forming a composite lubricating layer on a textured surface mainly includes burnishing, sputtering, and hot press sintering. Lubricants stored in textured micropatterns can supply the friction surface continuously, prolonging the service life of materials [19–24]. Therefore, the integration of LST and lubricants on the surface of materials is an effective means to achieve outstanding lubricating properties for the materials. However, few in-depth and systematic studies are available on the combination of laser surface texturing and bionic-laminated ceramics. These studies are necessary to investigate and improve the application limits of these laminated ceramic composites systematically.

On the basis of this background, two kinds of surface-lubricating structural-laminated ceramics with high reliability were designed and prepared. The three-dimensional lubricating layer fabricated on the ceramic surface realizes the integration of structure and lubricating function in laminated ceramic materials. This method can achieve outstanding lubricating properties and maintain the excellent mechanical properties of the ceramic. This process can also address the special

lubrication and wear failure in mechanical system under corrosive environment and wide-temperature range conditions, respectively. These materials are surface textured integrated with diamond-like carbon (DLC) film, LaF<sub>3</sub>-doped MoS<sub>2</sub> composite coating of alumina/nickel-laminated composites, and surface textured integrated with solid lubricants of alumina/molybdenum-laminated composites. These are suitable for use in a water environment and wide-temperature range conditions, respectively. The relation between the surface microstructure of the prepared materials and their properties (mechanical and tribological) was investigated.

---

## 9.2 Laser Surface Texturing and Tribological Properties of Ceramic Composites

Zirconia toughened alumina (ZTA) ceramic nanocomposites are potential candidates for the application of wear-resistant components because of their excellent properties, such as superior strength and fracture toughness, high wearability and hardness, low specific density, and antioxidation effect. Nevertheless, the friction coefficient and wear rate of ZTA nanocomposites are high under dry sliding conditions, which limit the application of these nanocomposites in tribological areas. LST is the basis for the integration of structured and lubricating functions in ceramics. The friction reduction mechanisms of surface texturing with different shapes and dimensions were investigated in several research works. The mechanisms mainly contain preventing stiction during start-up in magnetic storage industry, trapping wear debris in the texture micropatterns to reduce friction and wear, improving load capacity by enhancing hydrodynamic and hydrostatic lubrications, and acting as reservoirs to enhance lubricant retention and provide continuous lubrication to sliding surfaces [15, 25, 26]. The method is simple and effective in achieving antifriction and reduces the coefficient friction on the surface of ceramics by laser surface texturing. This part aims to reveal the microtexture mechanism that affects the tribological properties of ZTA nanocomposites and provide guidance for the optimum design of a composition-lubrication structure on the surface of laminated ceramic materials.

By controlling the sintering temperature properly, ZTA nanocomposites with excellent mechanical properties were prepared by hot pressing. The microhardness and bending strength of the sintered nanocomposites were approximately 17.01 GPa and 470 MPa, respectively. A commercial pulsed Nd:YAG laser was employed to produce the texture on the surface of the ZTA nanocomposites [27].

The scanning electron microscopy (SEM) photographs of the surface morphology of the ZTA nanocomposites with laser textures are presented in Fig. 9.1a. The 3D characteristic profiles of the textured surface for the nanocomposites are exhibited in Fig. 9.1b. A size-controlled microdimpled texture with a regular pattern was successfully fabricated on the surface of the ZTA nanocomposites by a pulsed Q-switch Nd:YAG solid-state laser. Through the optimized design of the laser texturing parameters, the tribological performance of the ZTA nanocomposites was significantly improved [27]. Figure 9.2 shows the curves of the friction coefficients of the

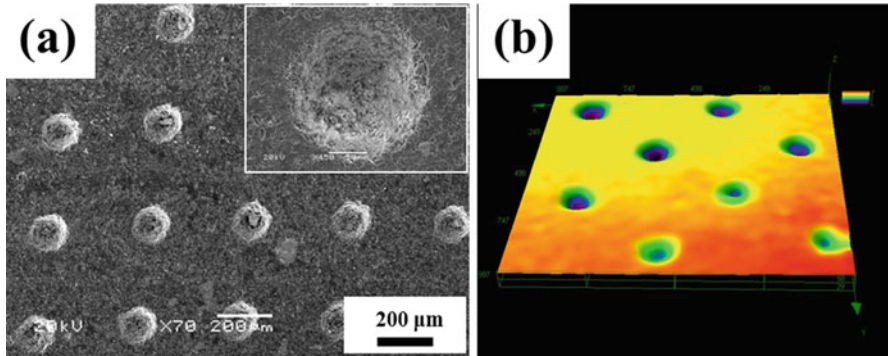


**Fig. 9.1** SEM photographs (a) and 3D characteristic profiles (b) of the textured surface for the nanocomposites

**Fig. 9.2** Friction coefficient under dry contact for untextured and textured surfaces with different densities [27]

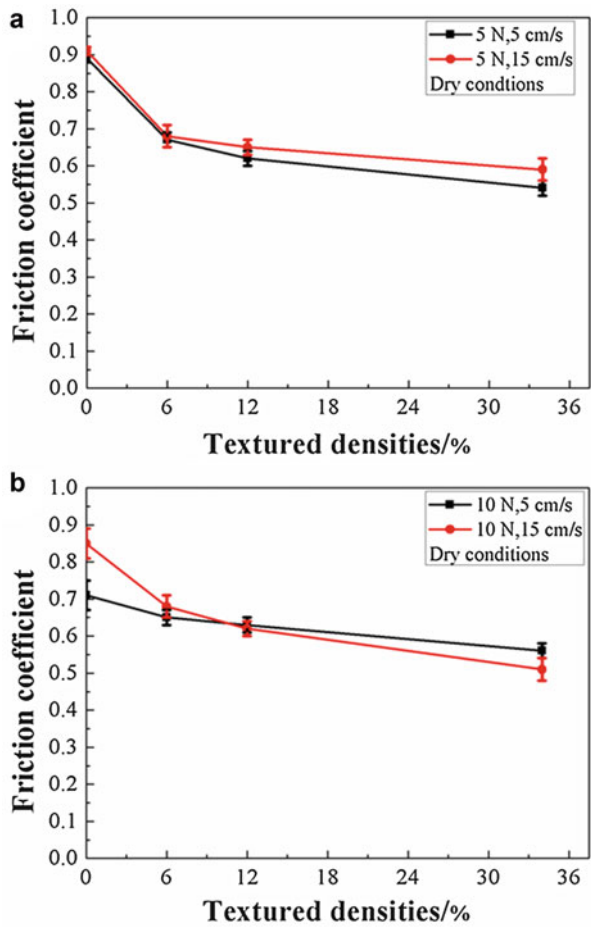
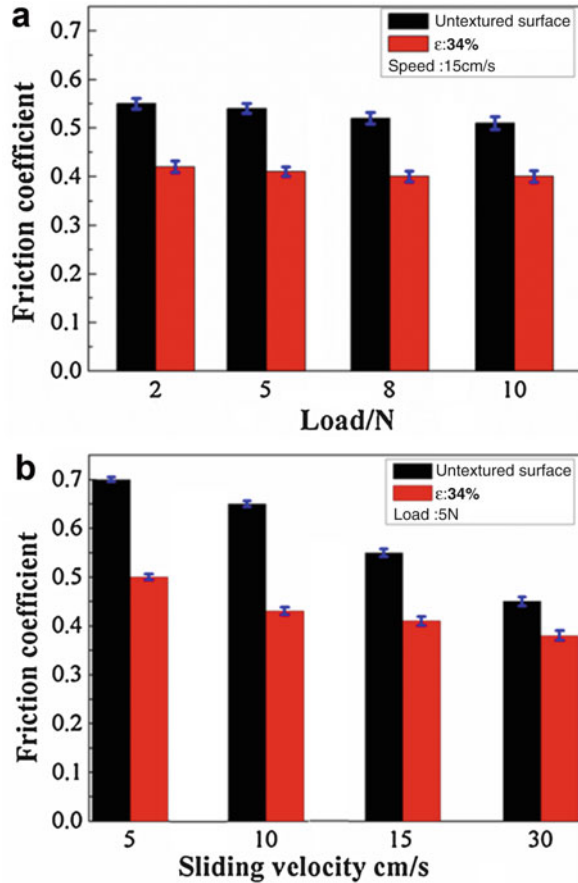


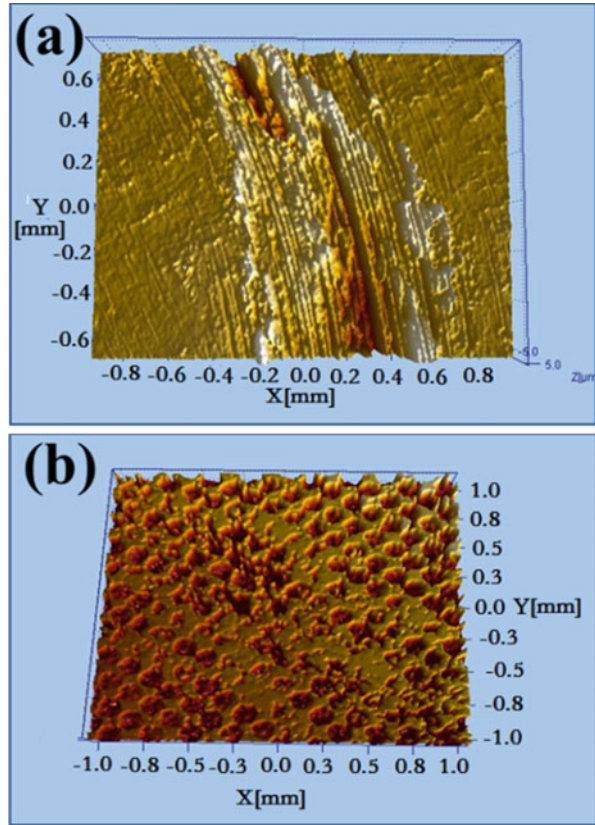
**Fig. 9.3** Average values of friction coefficient for the untextured and textured surfaces under different loads (a) and sliding velocities (b) under water lubrication [27]



untextured and textured surfaces of the ZTA nanocomposites under dry contact. The results indicated that the textured ZTA nanocomposite surface exhibited a low coefficient under dry friction conditions, especially under a relatively high load and sliding speed. Moreover, the texture density has an important effect on the property of the materials. The dense micro-dimples were advantageous in improving the tribological properties of the material. When the texture density is 34%, the friction coefficient of the textured ZTA nanocomposites can be reduced to 0.5. This value was approximately 44% lower than that of the untextured ZTA nanocomposite surface.

Figure 9.3 shows the average values of the friction coefficients of the untextured and textured ZTA nanocomposite surfaces at different loads and sliding speeds in a water environment. The increase in texture density resulted in an increase in water storage capacity. Thus, the reduction of the friction coefficient was primarily

**Fig. 9.4** 3D topographical of the wear scars of the untextured (a) and textured  $\varepsilon = 34\%$  (b) surfaces



attributed to the secondary lubricating effect produced by the lubricant (water) stored in the microdimples of the ZTA nanocomposite surfaces.

Figure 9.4 shows the typical 3D topographical structure of the worn surfaces of the untextured (Fig. 9.4a) and textured (Fig. 9.4b) samples. As shown in Fig. 9.4a, the untextured surfaces exhibited serious plough and adhesion wear under dry condition. By contrast, the textured surfaces exhibited excellent antiwear ability. The wear debris was effectively trapped and stored by the produced microdimples. This phenomenon can prevent abrasive wear and reduce plowing of the friction surfaces.

The understanding of such mechanisms provides guidance for the optimized design of a composition-lubrication structure on the ceramic surface. The process also provides theoretical guidance and technology support for the application of new ceramic materials in the high-technology fields. Therefore, the following laser surface texturing technology is used to design the surface composition-lubrication structure of alumina-matrix-laminated composites.

### 9.3 Surface Lubricating Design, Fabrication, and Tribological Properties in a Water Environment of $\text{Al}_2\text{O}_3/\text{Ni}$ -Laminated Composites

The chemical resistance of lubricating ceramics is the ability of a material to resist the destructive effect of an aggressive environment. In addition to the properties of the corrosive medium, this ability depends also on the microstructure of the lubricating ceramic material and conditions of the corrosion process, especially in medium-material contact [28–30]. High-performance alumina-matrix lubricating ceramics are potential candidates for the application of wear-resistant components because of their high wearability and hardness, low specific density, and anti-oxidation effect. However, the ability to resist the corrosive environment, such as liquids (solution of acid, alkaline, salts, molten salts, glasses, slags and metals, water, and so on), is one of the most limited properties of materials in many industrial applications. Therefore, designing and fabricating alumina-matrix-laminated composites with excellent mechanical and tribological properties that are adapted to the corrosive environment is significant. The combination of the bionic design with corrosion-resistant weak interface and surface lubricating design suitable for corrosive environment of ceramic-matrix-laminated composites is a promising way to achieve the optimal integration of mechanical and tribological properties. In this section, a surface lubricating structural  $\text{Al}_2\text{O}_3/\text{Ni}$ -laminated ceramics was designed and fabricated with high reliability and suitable for use in a water environment; the material can achieve stable and effective lubrication under water-based corrosive environments [31, 32].

First,  $\text{Al}_2\text{O}_3/\text{Ni}$ -laminated composites with excellent mechanical properties were successfully fabricated through layer-by-layer pressing and hot-press sintering method. Their bending strength, fracture toughness, and work of fracture can reach up to 470 MPa,  $9.6 \text{ MPa}\cdot\text{m}^{1/2}$ , and  $1952 \text{ J}\cdot\text{m}^{-2}$ , respectively [31]. On the basis of the  $\text{Al}_2\text{O}_3/\text{Ni}$ -laminated composites, two types of surface composition-lubrication structures were fabricated through the laser texturing and deposition/spraying technologies [31, 32]. These methods improved the surface tribological performance of the  $\text{Al}_2\text{O}_3/\text{Ni}$ -laminated composites under water environment remarkably. The regularity of the internal relationships between the surface texture micropattern and the microstructure, chemical composition, and properties of the lubricating films was systematically investigated. This process provided an important theoretical and experimental basis for the design of materials for water-based corrosive environments. The schematic and design concept of the surface composition-lubrication structure on the surface of  $\text{Al}_2\text{O}_3/\text{Ni}$ -laminated composites is shown in Fig. 9.5.

The microstructures of typical  $\text{Al}_2\text{O}_3/\text{Ni}$ -laminated composites are illustrated in Fig. 9.6, where the dark layer is the  $\text{Al}_2\text{O}_3$  layer and the light layer is the Ni, which is markedly thinner than the  $\text{Al}_2\text{O}_3$  layer. The laminated composites present a relatively straight obvious multilayer structure. The boundary between the strong/weak layer was sharp and without clear delamination (Figs. 9.6a, b). Moreover, the  $\text{Al}_2\text{O}_3$  and Ni layers in the composites were all fully densified because of their good sinterability. Thus, Ni and  $\text{Al}_2\text{O}_3$  presented compact-crystallized structures with no obvious



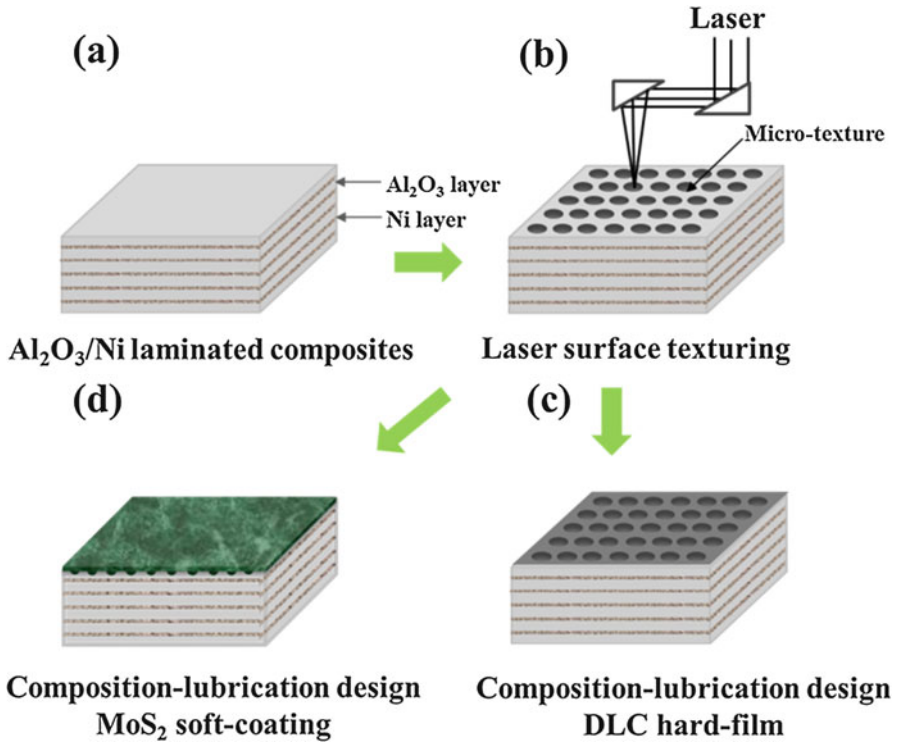


**Fig. 9.5** The schematic and surface lubricating design concept of Al<sub>2</sub>O<sub>3</sub>/Ni-laminated composites

flaws (Fig. 9.6c). These special weak interfacial layers played an important role in improving the mechanical and tribological properties of the laminated composites.

The SEM microtexture photographs of DLC films and LaF<sub>3</sub>-doped MoS<sub>2</sub> composite coatings of the Al<sub>2</sub>O<sub>3</sub>/Ni-laminated composites are presented in Fig. 9.7a and b, respectively. As seen from Fig. 9.7a, the microdimples of DLC films are uniform. The surface around the microdimples is smooth, indicating the absence of notable cracks or other morphological discontinuities. As seen from Fig. 9.7b, the LaF<sub>3</sub>-doped MoS<sub>2</sub> composite coatings on the textured surfaces are composed of closely packed powder particles. No obvious microcracks, holes, or other defects can be observed on the textured LaF<sub>3</sub>-doped MoS<sub>2</sub> composite coatings. The LaF<sub>3</sub>-doped MoS<sub>2</sub> composite coatings on the textured surface exhibit a relatively rough surface morphology.

Fig. 9.8a shows the different surface types of friction behaviors of Al<sub>2</sub>O<sub>3</sub>/Ni-laminated composites. The textured DLC films with different microdimple area densities are illustrated in Fig. 9.8b. The synergistic effect of a surface texture and DLC film in a water environment is a dominant cause of the decrease of the surface friction coefficient of the material. When friction against a stainless steel pin occurs in a water environment, the friction coefficient of the composition-lubrication structure can decrease to 0.06. This value is nearly one order of magnitude lower

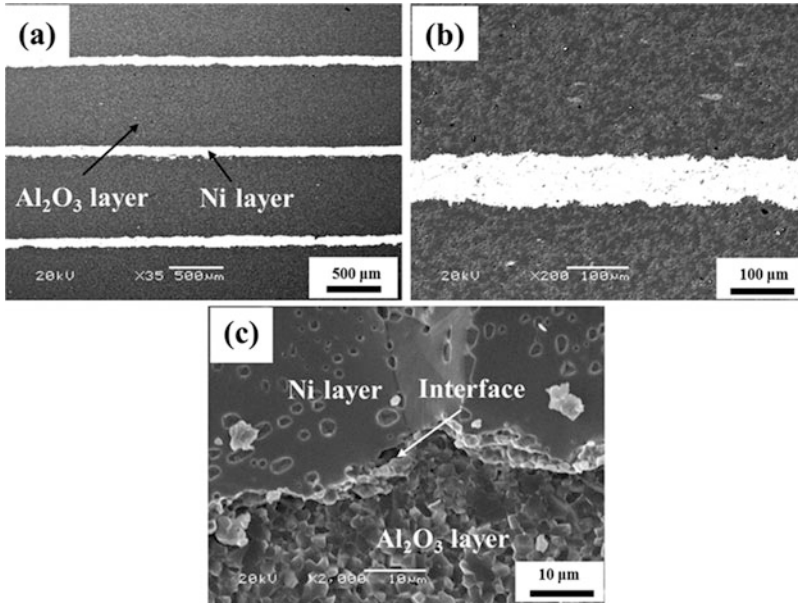


**Fig. 9.6** Multilayer and cross-section microstructure of the  $\text{Al}_2\text{O}_3/\text{Ni}$ -laminated composites

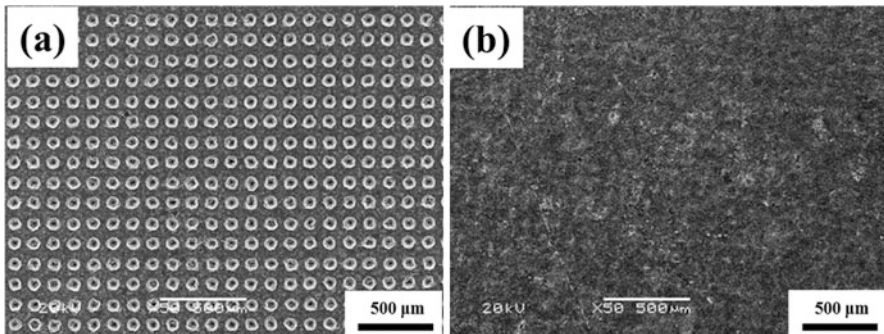


**Fig. 9.7** Textured surface lubricating structure with (a) DLC films and (b)  $\text{LaF}_3$ -doped  $\text{MoS}_2$  composite coating of the  $\text{Al}_2\text{O}_3/\text{Ni}$ -laminated composites

than that of the uncoated smooth ceramic surface (0.51). Moreover, the microdimple density of the texture with DLC film plays a key role in improving the tribological properties. When the texture density is low, the tribological properties of the composition-lubrication structure primarily depend on the synergistic lubrication of the surface texture and the DLC thin film because of the low storage of lubricant in the microdimples and the low viscosity feature of water. For high-density textured surfaces, the increase of texture density decreases with DLC content on the surface. This phenomenon indicates that the lubrication effect of DLC decreases. Meanwhile,

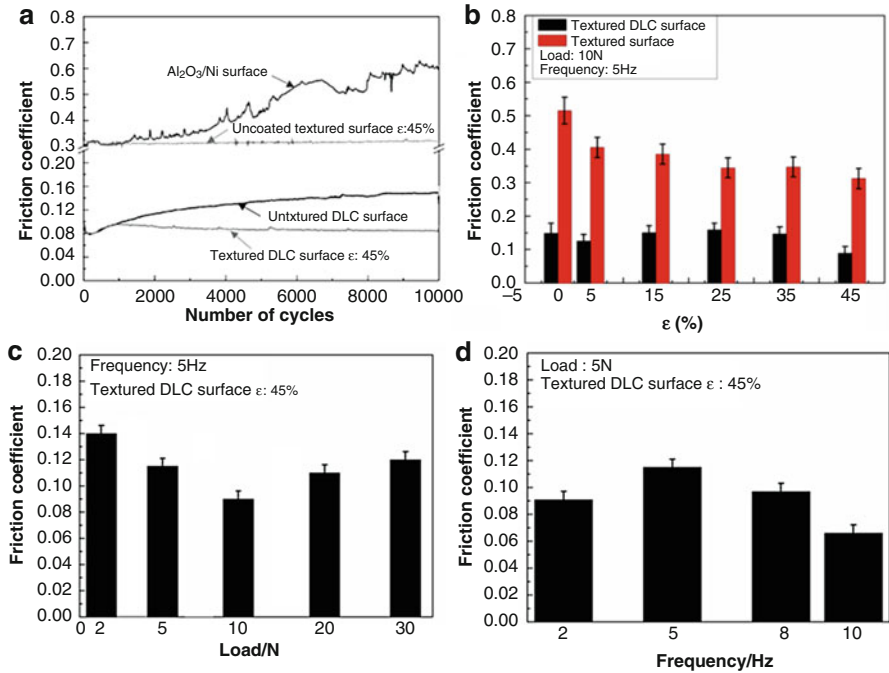


**Fig. 9.8** Friction coefficient curves (a) and the average values friction coefficients (b, c, d) of samples [31]

the increase of the texture density increases the storage volume of the lubricant that facilitates the formation of lubricating films on the friction surface. When the texture density is 5% or 45%, the composition-lubrication structure exhibits optimal tribological properties and adequate environmental adaptability. Figure 9.8c and d shows the average evolution values of the friction coefficients of the high-density (45%) textured DLC films at different loads and sliding frequencies under water lubrication. As shown in the figure, the textured DLC surface with a microdimple density of 45% exhibits excellent tribological properties in these working conditions. The friction coefficient of the textured surfaces is in the range of 0.06–0.14. The test conditions exhibited a significant effect on the tribological properties of the materials. The effect of sliding frequency on the friction coefficients was larger than the effect of the load.

Figure 9.9 shows the typical SEM micrographs of the worn surfaces of the untextured surface of DLC films (Fig. 9.9a) and textured surface of DLC films (Fig. 9.9b). As shown in Fig. 9.9a, the DLC films on the untextured substrate are severely worn out and flaked off, whereas the textured DLC films are intact and merely exhibit a very small abrasion at the edge of the microdimples (Fig. 9.9b). Therefore, the textured surfaces effectively prevented the peeling of DLC films and exhibited excellent antiwear ability. The performance of the Al<sub>2</sub>O<sub>3</sub>/Ni-laminated composites can be improved significantly by introducing a regular texture and DLC

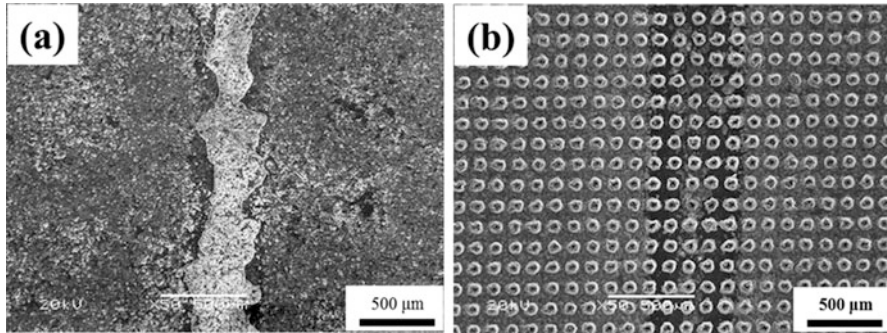


**Fig. 9.9** SEM morphologies of the wear tracks of untextured (a) and textured DLC films

films on the surface of the materials. Thus, low and stable friction coefficients can be obtained on the sliding surface.

For the soft composition-lubrication layers of  $\text{LaF}_3$ -doped  $\text{MoS}_2$  composite coatings on the surface of  $\text{Al}_2\text{O}_3/\text{Ni}$ -laminated composites, the following results were can be determined through the systematic investigation of the tribological behavior and fatigue failure mechanism in a water environment. Surface texture can significantly reduce the contact angle between the surfaces of  $\text{Al}_2\text{O}_3/\text{Ni}$ -laminated composites. The lubricant of water promoting the formation of water film and reducing the friction coefficient of the friction pair surfaces effectively. The friction coefficient of the soft composite lubrication surface can be reduced to 0.08, which is less than one-sixth of that of the smooth surface. The sliding lifetime of the lubricating coating can be increased by a factor of more than  $10^5$  cycles because of the self-locking function of the surface microtexture on the adhesive coating and its secondary lubrication effect, as shown in Fig. 9.10.

The typical SEM morphologies of the wear tracks of untextured and textured  $\text{LaF}_3$ -doped  $\text{MoS}_2$  composite coatings are shown in Fig. 9.11. The untextured  $\text{LaF}_3$ -doped  $\text{MoS}_2$  composite coating surface has flaked off completely resulting in severe wear off. However, for the sample with textured  $\text{LaF}_3$ -doped  $\text{MoS}_2$  composite coating surface, some  $\text{LaF}_3$ -doped  $\text{MoS}_2$  composite lubricants still exist in the sliding area and in microdimples though the coating has flaked off of local region. The  $\text{LaF}_3$ -doped  $\text{MoS}_2$  lubricants in microdimples can be continually replenished into the sliding surface when the coating on the wear scar is quickly worn off. This phenomenon will provide further lubrication.

#### **9.4 Surface Lubricating Design, Fabrication, and Tribological Properties Under a Wide-Range Temperature of $\text{Al}_2\text{O}_3/\text{Mo}$ -Laminated Composites**

The rapid development in aerospace, military industry, and other high-tech fields has resulted in the increasing demands for high-temperature wear-resistant materials and high-temperature self-lubricating technology. Self-lubricating composites with

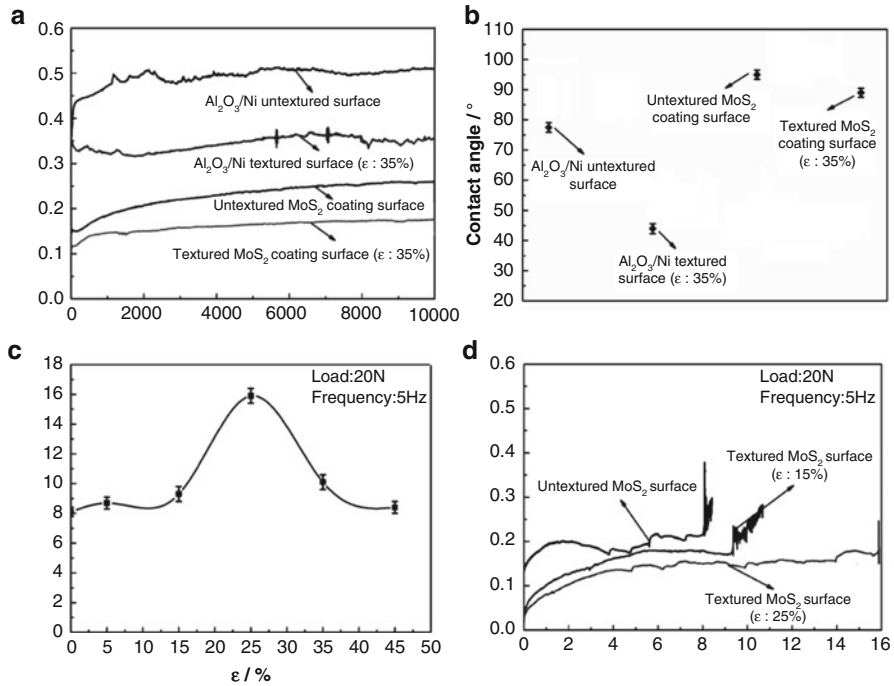


**Fig. 9.10** The friction curves (a) and the contact angles of water droplets (b) on material surface at a normal load of 10 N and the sliding frequency of 5 Hz; the wear life (c) and typical friction curves (d) of LaF<sub>3</sub>-doped MoS<sub>2</sub> composite coatings with different microdimpled densities at a normal load of 20 N and the sliding frequency of 5 Hz [32]

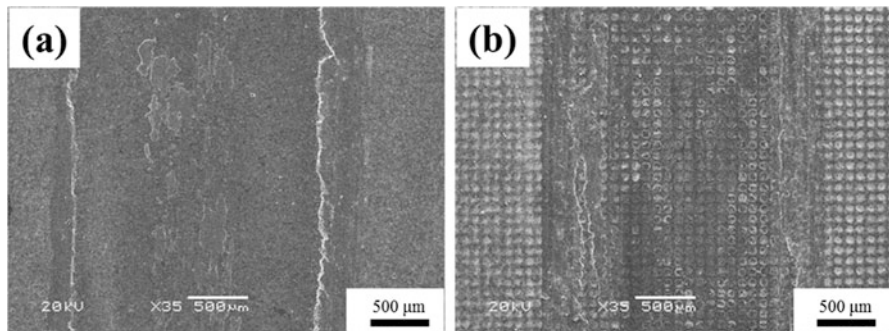


**Fig. 9.11** The typical SEM morphologies of the wear tracks of LaF<sub>3</sub>-doped MoS<sub>2</sub> composite coatings for untextured surface (a) and textured surface (b) after worn-out

excellent tribological performance in a wide-temperature range are urgently needed. However, lubricating materials are highly sensitive to temperature. The preparation of self-lubricating composites with wide-temperature range lubrication is very challenging and meaningful. Mechanical lubrication at temperatures above 400 °C

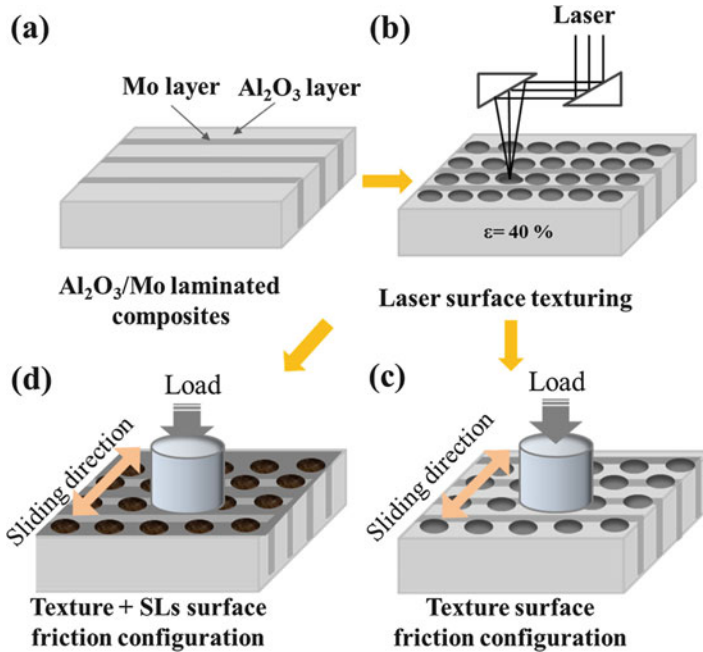


**Fig. 9.12** The schematic and surface lubricating design concept of Al<sub>2</sub>O<sub>3</sub>/Mo-laminated composites

can only depend on solid lubricants (SLs). Thus, two or three SLs are usually combined. Moreover, their synergy lubrication effect is fully utilized to achieve materials with wide-temperature range lubrication. In this part, we developed a three-dimensional lubricating layer by combining the optimized surface textures and SLs. Texture patterns were used as storage carrier of SLs. This structure can realize continuous lubrication from room temperature to 800 °C by fully utilizing the synergy effect and antifriction of the surface texture and SLs stored in the micro-dimples. Two types of different textured density surfaces and the three-dimensional lubricating layer with combined laser surface texture and solid film lubricant of Al<sub>2</sub>O<sub>3</sub>/Mo-laminated composites were fabricated. The synergy lubrication effect and mechanism of different lubricants from room temperature to 800 °C were discussed [33, 34]. The schematic and surface wide range lubricating design concept of Al<sub>2</sub>O<sub>3</sub>/Mo-laminated composites are shown in Fig. 9.12.

Using the LST technology, different microdimple densities and microgroove textures were fabricated on the surface of the Al<sub>2</sub>O<sub>3</sub>/Mo-laminated composites. Figure 9.13 shows the surface morphology of Al<sub>2</sub>O<sub>3</sub>/Mo-laminated composites with two types of microtextures and composite SLs. Clear and uniform micro-dimples and microgrooves with smooth edges are observed. The shape of the

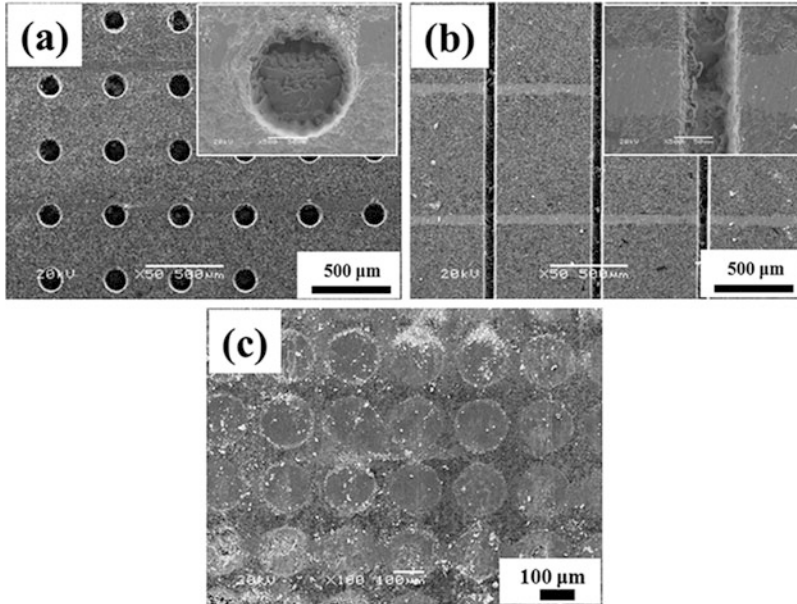


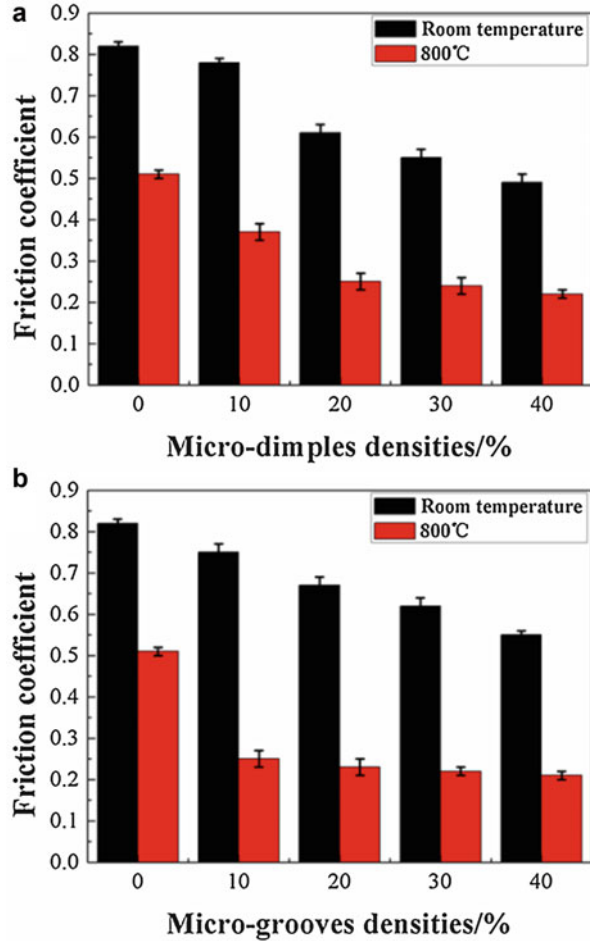
**Fig. 9.13** The surface morphology with microdimples (a), microgrooves (b), and burnished composite SLs (c) of  $\text{Al}_2\text{O}_3/\text{Mo}$ -laminated composites

microdimples is not influenced by the metal Mo layer (Figs. 9.13a, b). As shown in Fig. 9.13c, the textured microdimples are all filled with SLs after repeated wiping.

Figure 9.14 shows the friction coefficients of laser textured surfaces with different microdimple densities (a) and different microgroove densities (b) at room temperature and 800 °C. Considering the following advantages of the microtexture that increases the contact pressure of the friction surface, traps wear debris, and promotes the formation of lubricating film at high temperatures, the friction coefficients of  $\text{Al}_2\text{O}_3/\text{Mo}$ -laminated composites at 800 °C and at room temperature can be further reduced. Meanwhile, the friction coefficient of the material decreases with the increase in the texture surface density. At room temperature, the surface texture trapped wear debris. The friction coefficient of the surface texture can be decreased to as low as 0.5, which is 39% less than that of the untextured surface. Furthermore, the surface with a microdimpled texture exhibited a lower friction coefficient than that with a microgrooved texture. The surface texture facilitated an increase in the contact pressure of the friction pair and the contact area of the material surface with air at 800 °C. Thus, the formation and transfer of the lubricating film of  $\text{MoO}_3$  are facilitated. The friction coefficient can be reduced to as low as 0.22. This value is 55% less than that of the untextured surface.

Then, applying composite lubricants on the surface of optimized textured  $\text{Al}_2\text{O}_3/\text{Mo}$ -laminated composites and forming a surface three-dimensional lubricating layer can achieve the continuous lubrication of the material from room temperature to

**Fig. 9.14** Friction coefficients of laser textured surfaces with different microdimples densities (a) and different microgrooves densities (b) at room temperature and 800 °C [33]

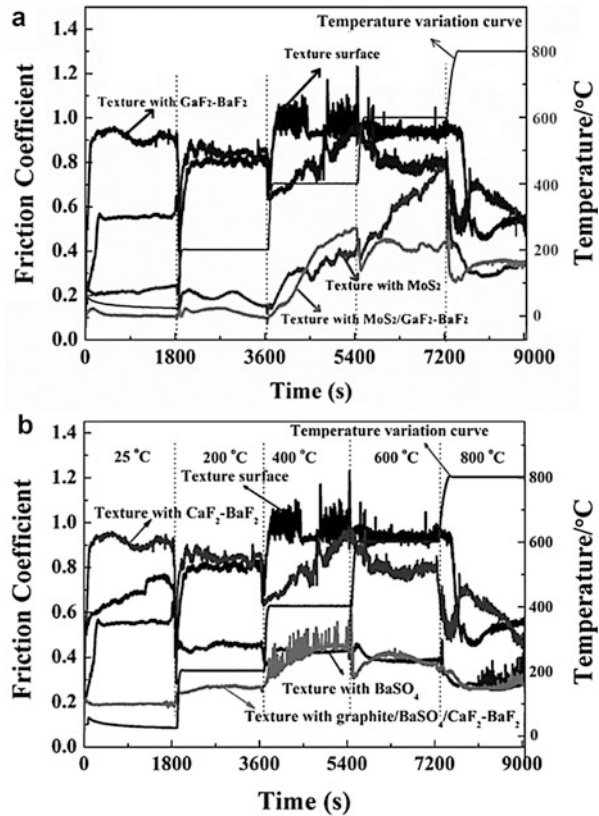


800 °C. Surface texture plays a key role in storing lubricants that can constantly lubricate the sliding surface during the friction process to form a continuous, uniform lubricating film. Therefore, the friction coefficient and wear of the sliding surface can be decreased, and the lifetime of the material can be effectively increased.

Herein, the three-dimensional structure combined with excellent antifriction and antiwear properties of solid lubricants with unique structural characteristics of microtexture effectively improved the tribological performance of materials at room temperature and up to increased temperatures. Therefore, the continuous lubrication of materials in a wide-temperature range can be sufficiently realized. For the surface of the  $\text{MoS}_2/\text{CaF}_2\text{-BaF}_2$  composite lubricants, the friction coefficients were below 0.50 throughout the entire temperature range. The lubrication effect was provided by  $\text{MoS}_2$  at a temperature range from room temperature to 600 °C. From 600 °C to 800 °C, the synergetic effects of  $\text{CaF}_2\text{-BaF}_2$  eutectic,



**Fig. 9.15** Friction coefficients of surface burnished with different solid lubricants from room temperature to 800 °C [34, 35]



CaMoO<sub>4</sub>, and BaMoO<sub>4</sub> effectively provided the lubrication effect. Composite graphite/BaSO<sub>4</sub>/CaF<sub>2</sub>-BaF<sub>2</sub> lubricants maintained the friction coefficient of materials below 0.45 in the entire tested temperature range from room temperature to 800 °C. The lubrication effect was provided by graphite, BaSO<sub>4</sub>, and the synergy effect of BaMoO<sub>4</sub> and CaMoO<sub>4</sub> at room, medium and high temperatures, respectively (Fig. 9.15).

Figure 9.16 shows the typical wear tracks of the untextured surface (Fig. 9.16a), textured without burnishing SLs (Figs. 9.16b, c), and textured surface with burnishing SLs at 800 °C under the same conditions. The untextured surface exhibited serious wear and plastic deformation mainly because of the temperature increase in the friction experiment. However, for the textured surface without burnishing SLs, trapping wear debris in the microgrooves and microdimples can be clearly observed. The texture also maintained relatively intact morphology. For the textured surface burnished with SLs, microdimples maintained relatively intact morphology. A mild wear surface was also produced after a long friction experiment. The SLs stored in microdimples were squeezed to the friction surface during friction process forming a continuous lubricating film.

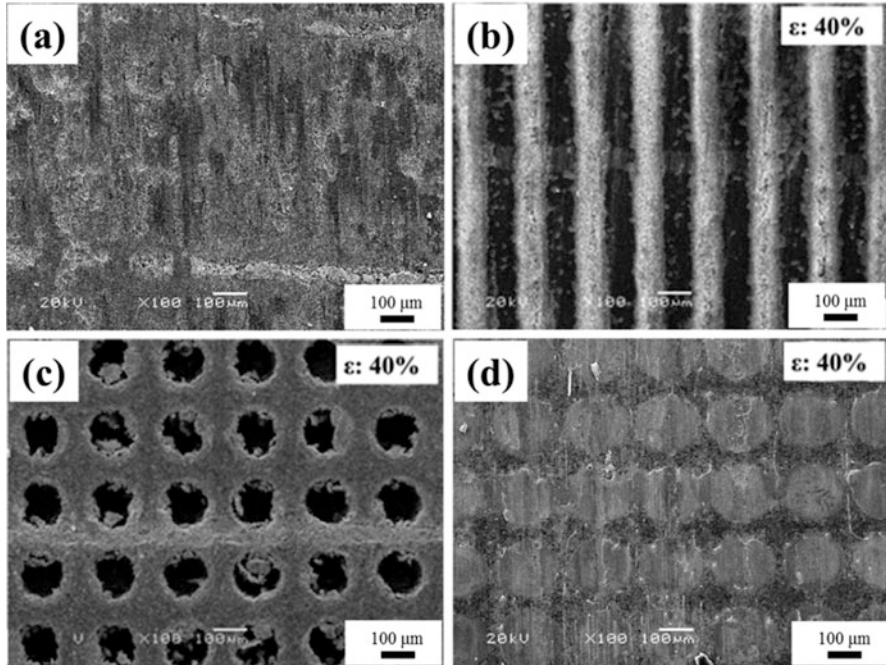


**Fig. 9.16** Worn surfaces of untextured surface (a), textured surfaces with microgrooves (b), microdimples (c) and textured surface with burnished SLs (d) at 800 °C

In summary,  $\text{Al}_2\text{O}_3/\text{Ni}$  and  $\text{Al}_2\text{O}_3/\text{Mo}$ -laminated composites with surface composition-lubrication structure realize the integration of mechanical and lubricating properties. The performance of the surface composition-lubrication layers can be facility controlled by the design of the texture micropattern, film/coating characteristics and compound of solid lubricants. The excellent mechanical and tribological properties of the optimal laminated and surface composition-lubrication structure enable them to be used in a wide range of applications. These methods also provided theories and technologies for the preparation and application of high performance lubricating materials that can be used in corrosive and wide-temperature range environments.

**Acknowledgment** This work was supported by the National Natural Science Foundation of China (51775534) and the Youth Innovation Promotion Association CAS (2013272).

## References

1. Zhang, Y.S., Hu, L.T., Chen, J.M., Liu, W.M.: Lubrication behavior of Y-TZP/ $\text{Al}_2\text{O}_3$ /Mo nanocomposites at high temperature. *Wear*. **268**(9–10), 1091–1094 (2010)
2. Hu, T.C., Zhang, Y.S., Hu, L.T.: Mechanical and wear characteristic of Y-TZP/ $\text{Al}_2\text{O}_3$  nanocomposites. *Ind. Lubr. Tribol.* **66**(2), 209–214 (2014)

3. Qi, Y.E., Zhang, Y.S., Hu, L.T.: High-temperature self-lubricated properties of  $\text{Al}_2\text{O}_3/\text{Mo}$  laminated composites. *Wear*. **280–281**, 1–4 (2012)
4. Fang, Y., Zhang, Y.S., Song, J.J., Fan, H.Z., Hu, L.T.: Design and fabrication of laminated-graded zirconia self-lubricating composites. *Mater. Des.* **49**, 421–425 (2013)
5. Qi, Y.E., Zhang, Y.S., Fang, Y., Hu, L.T.: Design and preparation of high-performance alumina functional graded self-lubricated ceramic composites. *Compos. Part B Eng.* **47**, 145–149 (2013)
6. Fang, Y., Zhang, Y.S., Song, J.J., Fan, H.Z., Hu, L.T.: Influence of structural parameters on the tribological properties of  $\text{Al}_2\text{O}_3/\text{Mo}$  laminated nanocomposites. *Wear*. **320**, 152–160 (2014)
7. Wang, C.A., Huang, Y., Zan, Q.F., Zou, L.H., Cai, S.Y.: Control of composition and structure in laminated silicon nitride/boron nitride composites. *J. Am. Ceram. Soc.* **85**(10), 2457–2461 (2002)
8. Hwu, K.L., Derby, B.: Fracture of metal/ceramic laminates-II. Crack growth resistance and toughness. *Acta Mater.* **47**(2), 545–563 (1999)
9. Wang, C.A., Huang, Y., Zan, Q.F., Guo, H., Cai, S.Y.: Biomimetic structure design—a possible approach to change the brittleness of ceramics in nature. *Mater. Sci. Eng. C*. **11**(1), 9–12 (2000)
10. Clegg, W.J., Kendall, K., Alford, N.M., Button, T.W., Birchall, J.D.: A simple way to make tough ceramics. *Nature*. **347**(6292), 455–457 (1990)
11. Zuo, K.H., Jiang, D.L., Lin, Q.L.: Mechanical properties of  $\text{Al}_2\text{O}_3/\text{Ni}$  laminated composites. *Mater. Lett.* **60**(9–10), 1265–1268 (2006)
12. Song, J.J., Zhang, Y.S., Fang, Y., Fan, H.Z., Hu, L.T., Qu, J.M.: Influence of structure parameters and transition interface on the fracture property of  $\text{Al}_2\text{O}_3/\text{Mo}$  laminated composite. *J. Eur. Ceram. Soc.* **35**, 1581–1591 (2015)
13. Ryk, G., Kligerman, Y., Etsion, I.: Experimental investigation of laser surface texturing for reciprocating automotive components. *Tribol. Trans.* **45**(4), 444–449 (2002)
14. Yu, X.Q., He, S., Cai, R.L.: Frictional characteristics of mechanical seals with a laser-textured seal face. *J. Mater. Process. Technol.* **129**(1–3), 463–466 (2002)
15. Etsion, I., Halperin, G., Brizmer, V., Kligerman, Y.: Experimental investigation of laser surface textured parallel thrust bearings. *Tribol. Lett.* **17**(2), 295–300 (2004)
16. Kawasegi, N., Sugimori, H., Morimoto, H., Morita, N., Hori, I.: Development of cutting tools with microscale and nanoscale textures to improve frictional behavior. *Precis. Eng. J. Int. Soc. Precis. Eng. Nanotechnol.* **33**(3), 248–254 (2009)
17. Baumgart, P., Krajnovich, D.J., Nguyen, T.A., Tam, A.C.: A new laser texturing technique for high-performance magnetic disk drives. *IEEE Trans. Magn.* **31**(6), 2946–2951 (1995)
18. Varenberg, M., Halperin, G., Etsion, I.: Different aspects of the role of wear debris in fretting wear. *Wear*. **252**(11–12), 902–910 (2002)
19. Etsion, I., Halperin, G.: A laser surface textured hydrostatic mechanical seal. *Tribol. Trans.* **45**(3), 430–434 (2002)
20. Kovalchenko, A., Ajayi, O., Erdemir, A., Fenske, G., Etsion, I.: The effect of laser surface texturing on transitions in lubrication regimes during unidirectional sliding contact. *Tribol. Int.* **38**(3), 219–225 (2005)
21. Hu, T.C., Zhang, Y.S., Hu, L.T.: Tribological investigation of  $\text{MoS}_2$  coatings deposited on the laser textured surface. *Wear*. **278–279**, 77–82 (2012)
22. Uehara, Y., Wakuda, M., Yamauchi, Y., Kanzaki, S., Sakaguchi, S.: Tribological properties of dimpled silicon nitride under oil lubrication. *J. Eur. Ceram. Soc.* **24**(2), 369–373 (2004)
23. Wang, X., Adachi, K., Otsuka, K., Kato, K.: Optimization of the surface texture for silicon carbide sliding in water. *Appl. Surf. Sci.* **253**(3), 1282–1286 (2006)
24. Schreck, S., Zum Gahr, K.H.: Laser-assisted structuring of ceramic and steel surfaces for improving tribological properties. *Appl. Surf. Sci.* **247**(1–4), 616–622 (2005)
25. Etsion, I., Kligerman, Y., Halperin, G.: Analytical and experimental investigation of laser-textured mechanical seal faces. *Tribol. Trans.* **42**(3), 511–516 (1999)
26. Etsion, I., Sher, E.: Improving fuel efficiency with laser surface textured piston rings. *Tribol. Int.* **42**(4), 542–547 (2009)

27. Fan, H.Z., Hu, T.C., Zhang, Y.S., Fang, Y., Song, J.J., Hu, L.T.: Tribological properties of micro-textured surfaces of ZTA ceramic nanocomposites under the combined effect of test conditions and environments. *Tribol. Int.* **78**, 134–141 (2014)
28. Hnatko, M., Galusek, D., Šajgalík, P.: Low cost preparation of  $\text{Si}_3\text{N}_4$ -SiC micro/nano composites by in-situ carbothermal reduction of silica in silicon nitride matrix. *J. Eur. Ceram. Soc.* **24**(2), 189–196 (2004)
29. Křesťan, J., Šajgalík, P., Pánek, Z.: Carbothermal reduction and nitridation of powder pyrophyllite raw material. *J. Eur. Ceram. Soc.* **24**(5), 791–796 (2004)
30. Balog, M., Šajgalík, P., Lenčák, Z., Kečkéš, J., Huang, J.T.: Liquid phase sintering of SiC with AlN and rare-earth oxide additives, silicon-based structural ceramics for the new millennium. Brito ME, Lin HT, Plucknett K (Eds.) *Ceram. Trans.* **142**, 191–202 (2003)
31. Fan, H.Z., Zhang, Y.S., Hu, T.C., Song, J.J., Ding, Q., Hu, L.T.: Surface composition-lubrication design of  $\text{Al}_2\text{O}_3/\text{Ni}$  laminated composites—Part I: tribological synergy effect of micro-dimpled texture and diamond-like carbon films in a water environment. *Tribol. Int.* **84**, 142–151 (2015)
32. Fan, H.Z., Hu, T.C., Wan, H.Q., Zhang, Y.S., Song, J.J., Hu, L.T.: Surface composition-lubrication design of  $\text{Al}_2\text{O}_3/\text{Ni}$  laminated composites – Part II: tribological behavior of  $\text{LaF}_3$ -doped  $\text{MoS}_2$  composite coating in a water environment. *Tribol. Int.* **96**, 258–268 (2016)
33. Fang, Y., Zhang, Y.S., Fan, H.Z., Hu, T.C., Song, J.J., Hu, L.T.: Surface composition-lubrication design of  $\text{Al}_2\text{O}_3/\text{Mo}$  laminated composites – Part I: influence of laser surface texturing on the tribological behavior at 25 and 800 °C. *Wear.* **334–335**, 23–34 (2015)
34. Fang, Y., Fan, H.Z., Song, J.J., Zhang, Y.S., Hu, L.T.: Surface engineering design of  $\text{Al}_2\text{O}_3/\text{Mo}$  laminated composites – Part II: continuous lubrication effects of a three-dimensional lubricating layer at temperatures from 25 to 800 °C. *Wear.* **360–361**, 97–103 (2016)
35. Fang, Y., Fan, H.Z., Zhang, Y.S., Song J.J., Hu, L.T.: Preparation and tribological performance of three-dimensional lubricating layer on the surface of  $\text{Al}_2\text{O}_3/\text{Mo}$  self-lubricating structural ceramics. *Tribol.* **37**(3), 395–401 (2017 in Chinese)